Turkish Journal of Electrical Engineering & Computer Sciences

http://journals.tubitak.gov.tr/elektrik/

Research Article

Turk J Elec Eng & Comp Sci
(2017) 25: 1048 – 1058

doi:10.3906/elk-1503-189

Design and analysis of a reduced ultrawideband band-notched band-pass filter

Navid DARYASAFAR[1,*], Mojtaba TANGAKI[2], Mohammad Naser MOGHADASI[3], Ramazanali SADEGHZADEH[4]

[1]Department of Electrical Engineering, Dashtestan Branch, Islamic Azad University, Dashtestan, Iran
[2]Department of Electrical Engineering, Bushehr Branch, Islamic Azad University, Bushehr, Iran
[3]Faculty of Engineering, Science and Research Branch, Islamic Azad University, Tehran, Iran
[4]Faculty of Electrical Engineering, K.N. Toosi University of Technology, Tehran, Iran

Received: 20.03.2015 • **Accepted/Published Online:** 19.03.2016 • **Final Version:** 10.04.2017

Abstract: In this paper we intend to design a reduced ultrawideband band-pass filter using new models of coupled transmission lines. In this paper, by providing a new model of resonators, the bandwidth of band-pass filters (which are among the most crucial elements in communication systems) will be moderately increased, while their size and volume decreases. According to the change of their equations and consequent changes in basic parameters of these models, optimization and dependency among these parameters and also the frequency response of these filters will be developed to utilize notches in the pass-band, and a reduced ultrawideband band-pass filter with notch will be designed and analyzed.

Key words: Multiple-mode resonator, stepped-impedance resonator, band-pass filter, reduced notched ultrawideband

1. Introduction

In this paper, before presenting new models of coupled transmission lines it is necessary to present and analyze the general method of designing band-pass filters. According to the general method of designing band-pass filters in [1], using the template of integrated elements, first a low-pass filter is designed and then the equivalent band-pass filter that uses coupled transmission lines will be designed and analyzed. Figure 1 shows a primary example of a low-pass filter [1].

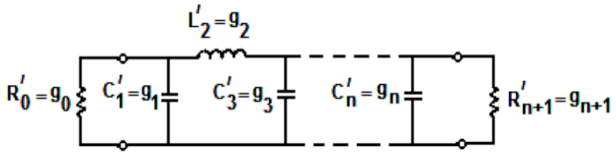

Figure 1. Circuit model and primary template of a low-pass filter [1].

In order to acquire the parameters and integrated elements of a band-pass filter at the resonance frequency w_0 based on the parameters and integrated elements of a low-pass filter according to its parallel or serial structure, two different parameters will be defined. One of the parameters, which is defined at the central resonance frequency of the filter, is the slope parameter. For any serial resonator the reactance slope parameter

*Correspondence: navid_daryasafar@yahoo.com

is defined by Eq. (1) [1].

$$\alpha = \frac{\omega_0}{2}\frac{dX}{d\omega}|\omega_0 \quad \Omega \tag{1}$$

In Eq. (1), X is the reactance of the resonator.

Similar to this parameter, for a parallel resonator the susceptance slope parameter is defined by Eq. (2) [1].

$$\gamma = \frac{\omega_0}{2}\frac{dX}{d\omega}|\omega_0 \tag{2}$$

In Eq. (2), B is the parallel resonator's susceptance. After designing the low-pass filter and determining the integrated elements used in its circuit model, the circuit model of the band-pass filter can be obtained using the primary template. As can be observed in Figure 2, in the circuit model of the band-pass filter derived from the primary template of the low-pass filter, parallel and serial resonators have been used. In order to calculate the values of the integrated elements in the parallel and serial resonators, the circuit model of the band-pass filter that has been designed based on the values of the integrated elements used in the primary template of a low-pass filter, the reactance, and susceptance slope parameters are used.

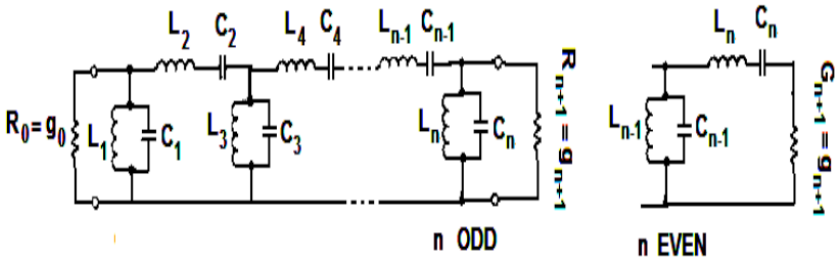

Figure 2. Circuit model of the band-pass filter derived from the primary template of a low-pass filter.

The equations that present the relations between the integrated elements of the band-pass and low-pass filters for parallel and serial resonators are as follows:

$$\gamma_i = \omega_0 C_j = \frac{1}{\omega_0 L_j} = \frac{\omega_1' g_j}{W} \tag{3}$$

$$\alpha_K = \omega_0 L_K = \frac{1}{\omega_0 L_j} = \frac{\omega_1' g_K}{W} \tag{4}$$

In Eqs. (3) and (4), W is the relative bandwidth and w_0 is the central resonance frequency for the band-pass filter.

Multiple-mode resonators (MMRs) and stepped-impedance resonators (SIRs) are two of the most used resonators in the design of broadband band-pass filters. The new model proposed in this study is an improved model of these two resonators.

The main frequency and the frequencies created by the harmonics of the resonances of higher frequencies are used in the creation of stop-band in ultrawide bandwidths. Eqs. (5) and (6) present these frequencies.

$$\theta_{01} = \tan^{-1}\left(\sqrt{\frac{K_1 K_2}{K_1 + K_2 + 1}}\right) \tag{5}$$

$$\theta_{02} = \tan^{-1}\left(\sqrt{\frac{K_1 + K_1K_2 + 1}{K_2}}\right) \tag{6}$$

In these equations, θ_{01} and θ_{02} are the corresponding phase shifts resulting at the notch frequencies along the lambda length in the band-stop filter of a MMR and the parameters K_1 and K_2 are the impedance ratios of different parts of the resonator.

In the design of the proposed filter and with an accurate mathematical analysis, the relations of main and higher frequencies with K parameters were studied, and thus the location of the stop-band within the ultrawide bandwidth will be determined in order to be able to optionally adjust the stop-band.

2. Broadband band-pass filters in recent studies

The two band-pass filters that will be studied in this paper are from the most recent research done in the past few years. One of them has been designed using SIRs and the other has been designed using MMRs. It must be noted that the greatest deficiency of these two filters is the lack of a notch.

2.1. Three-section MMR

Some of the most important resonators that have gained the attention of designers of passive microwave elements are MMRs, and many band-pass filters have been designed based on these resonators [2–6]. Figure 3 shows the structure of a MMR, which is the main resonator used in the design of such broadband filters.

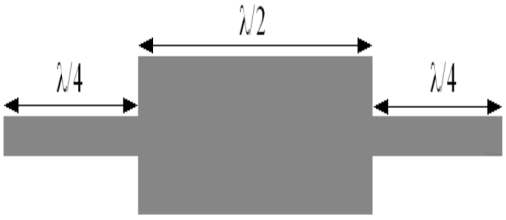

Figure 3. The structure of a MMR.

In the next step, based on the MMR presented in Figure 3, a broadband band-pass filter that has been designed and proposed will be simulated. Figure 4 shows the structure of this band-pass filter designed based on the MMR.

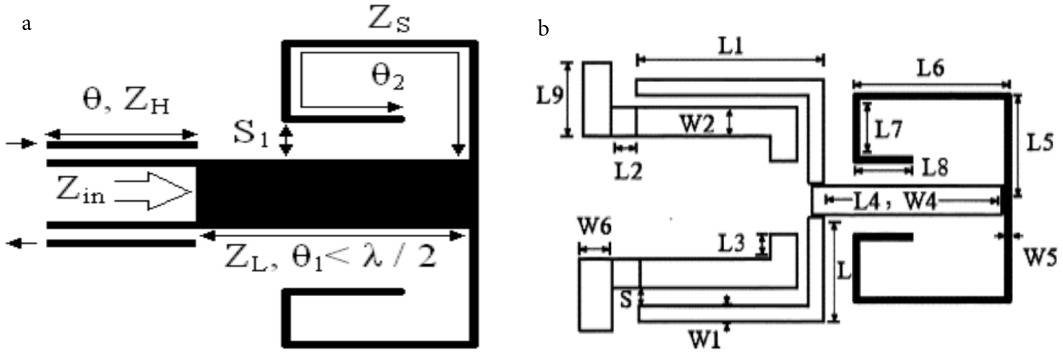

Figure 4. a) Structure of the band-pass filter designed based on the MMR shown in Figure 3, b) the structure based on optimized values.

As can be observed from the structure of the band-pass filter presented in Figure 4, the presented filter includes one MMR and two coupling sections where the length of the coupling lines is equal to the two lateral sections of the filter. Similarly to the band-pass filter designed using SIRs in the next section, the structure of the filter presented in Figure 4 will first be implemented in the S-parameters workspace.

After implementing the structure of this filter, all of its parameters will be selected in order to have an acceptable frequency response in the ADS software based on the values given in Table 1.

Table 1. Optimized values of the given broadband band-pass filter.

Parameter	L	L_1	L_2	L_3	L_4	L_5
Value	1.2 mm	8.59 mm	0.3 mm	0.6 mm	5.4 mm	5.4 mm
Parameter	L_6	L_7	L_8	L_9	W_1	W_2
Value	4.1 mm	3.36 mm	1.7 mm	2.74 mm	0.2 mm	0.44 mm
Parameter	W_4	W_5	W_6	S	S_1	
Value	1.1 mm	0.1 mm	1.6 mm	0.08 mm	0.24 mm	

After selecting the optimized values for the parameters of the designed filter, its structure will be taken to the workspace of the program. Figure 5 shows the structure of this broadband band-pass filter designed using a MMR in the workspace of the ADS program.

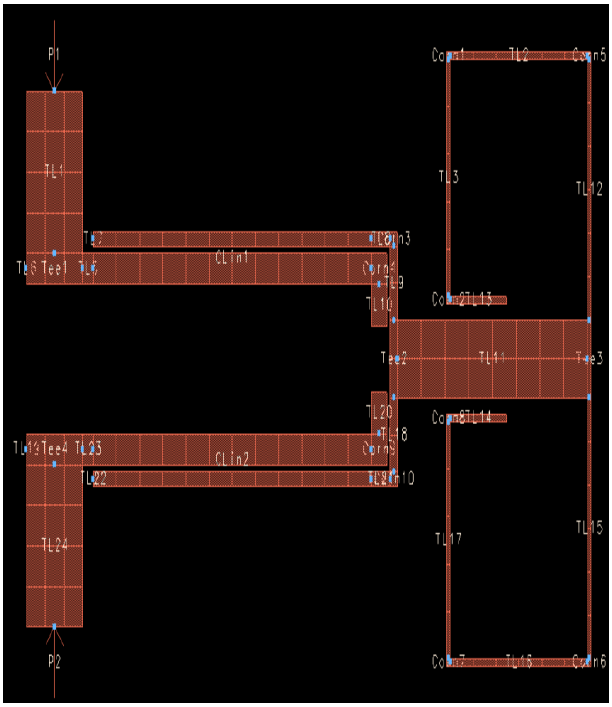

Figure 5. Structure of the broadband band-pass filter designed using a MMR in the workspace of the ADS program.

After implementing the filter, the structure of this filter is implemented on a substrate with a thickness of 0.508 mm and dielectric constant of 2.2 and the frequency response is simulated in the range of 0–16 GHz.

Figure 6 shows the simulated frequency response of the broadband band-pass filter designed using a MMR in the workspace of ADS versus return losses (S_{11}) and insertion losses (S_{21}) in a range of 0–16 GHz.

2.2. Two-section SIR

Another important resonator that has been studied by designers of passive microwave elements is the SIR [7–9].

The broadband band-pass filter designed in [7] is chosen. Figure 7 shows the structure of the asymmetric two-section SIR used in this reference.

Figure 8 shows the structure and model of the broadband band-pass filter presented in [7].

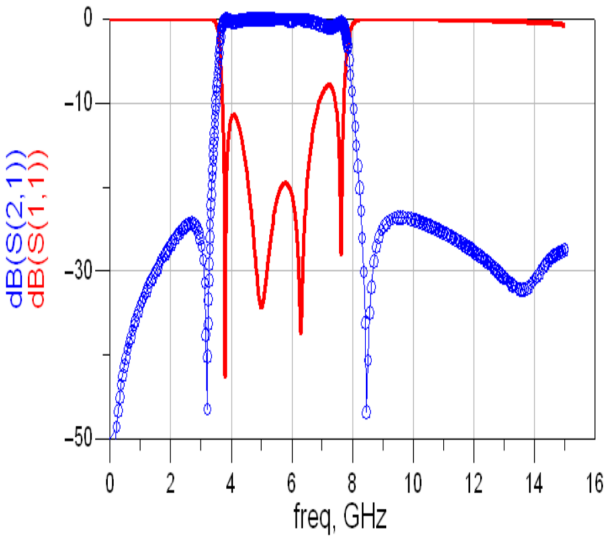

Figure 6. The simulated frequency response of the broadband band-pass filter designed using a MMR in the workspace of ADS versus return losses (S_{11}) and insertion losses (S_{21}) in a range of 0–16 GHz.

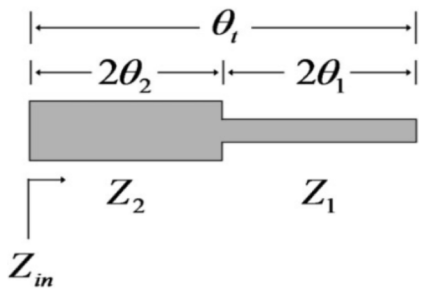

Figure 7. Structure of the asymmetric two-section SIR used in reference [7].

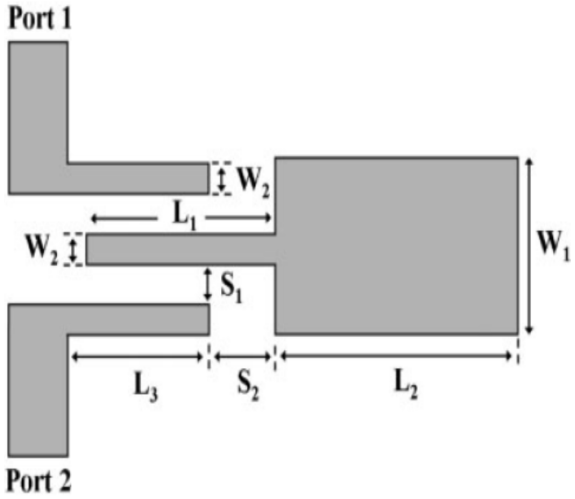

Figure 8. Structure and model of the broadband band-pass filter presented in reference [7].

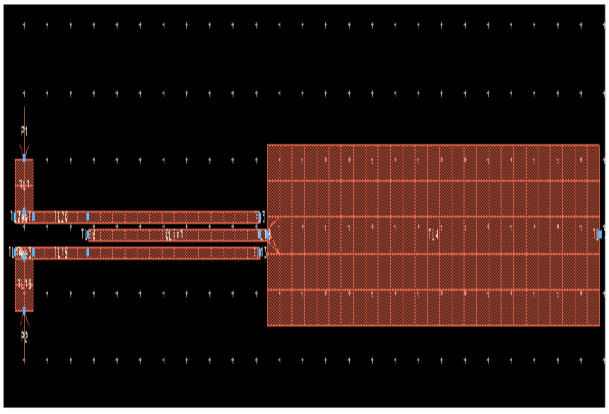

Figure 9. Structure of the broadband band-pass filter of reference [7] in the workspace of ADS.

In [7] and based on the structure presented in Figure 8, a broadband band-pass filter has been designed, analyzed, and built. The structure of this filter has been implemented on a Duroid 5880 substrate with a thickness of 0.787 mm and a dielectric constant of 2.2.

Figure 9 shows the implemented broadband band-pass filter using values given in Table 2 in the S-parameters workspace of the ADS program, which has been formed using 15 microstrip transmission lines.

Table 2. Optimized values for the broadband band-pass filter given in [7].

Parameter	L_1	L_2	L_3	W_1	W_2	S_1	S_2
Value	9.8 mm	18.2 mm	13.4 mm	3.4 mm	0.2 mm	0.14 mm	0.4 mm

After implementing the filter in the workspace of ADS, the structure of this filter is implemented on a substrate with a thickness of 0.787 mm and a dielectric constant of 2.2 and then the frequency response in the range of 0–7 GHz is simulated.

Figure 10 shows the frequency response of the simulated filter in the (S_{11}) and insertion losses (S_{21}) in the range of 0–16 GHz.

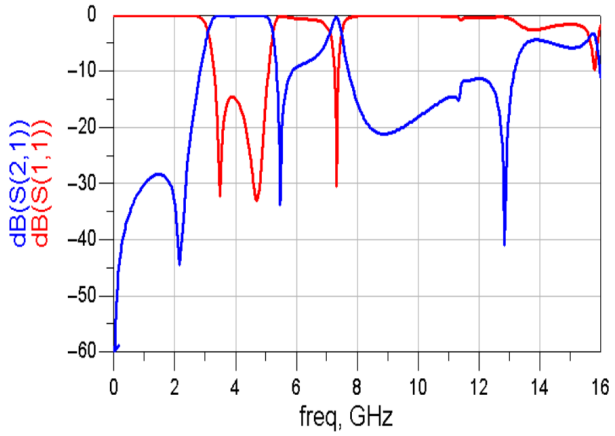

Figure 10. Frequency response of the simulated filter in the workspace of ADS plotted versus return losses (S_{11}) and insertion losses (S_{21}) in the range of 0–16 GHz.

As can be observed in the frequency response of the filter simulated using ADS versus return losses (S_{11}) and insertion losses (S_{21}) in the range of 0–16 GHz shown in Figure 10, this filter has the first harmonic at about 7.5 GHz, which limits the stop-band of this filter and therefore this filter cannot be used for applications that require greater stop-bands.

3. Simulation of the structure of the broadband band-pass filter

As shown in Figure 11, the structure of the band-pass filter includes a two-section SIR, in which the first section is similar to the first section of regular SIRs and the second section has two equal parallel branches. Figure 11 shows the structure of this resonator without a notch, which uses the combination of two transmission lines with a length of $\lambda/4$ as feed lines. Generally the structure combined with these feed lines will provide a wideband band-pass filter.

The optimized values of the broadband band-pass filter are given in Table 3. As given in this table, the filter is divided into 6 transmission lines.

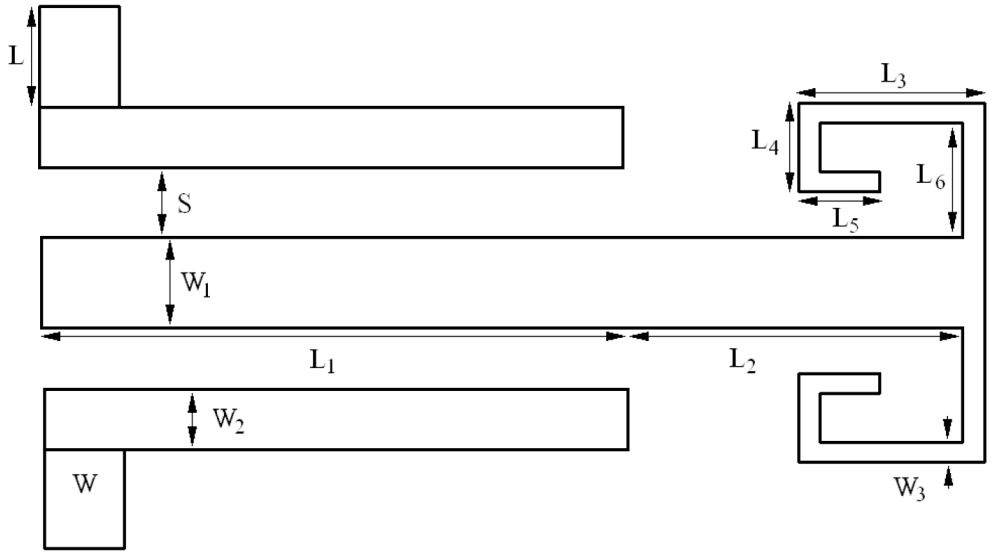

Figure 11. Structure of the broadband band-pass filter.

Table 3. Optimized values of the broadband band-pass filter.

Parameter	L	L_1	L_2	L_3	L_4	L_5
Value	1 mm	10 mm	4 mm	3.6 mm	0.9 mm	1 mm
Parameter	W	W_1	W_2	W_3	S	L_6
Value	1 mm	0.3 mm	0.28 mm	0.2 mm	0.1 mm	1.2 mm

Figure 12 shows another type of these kinds of band-pass filters with notches based on the optimized parameters, shown using the ADS program.

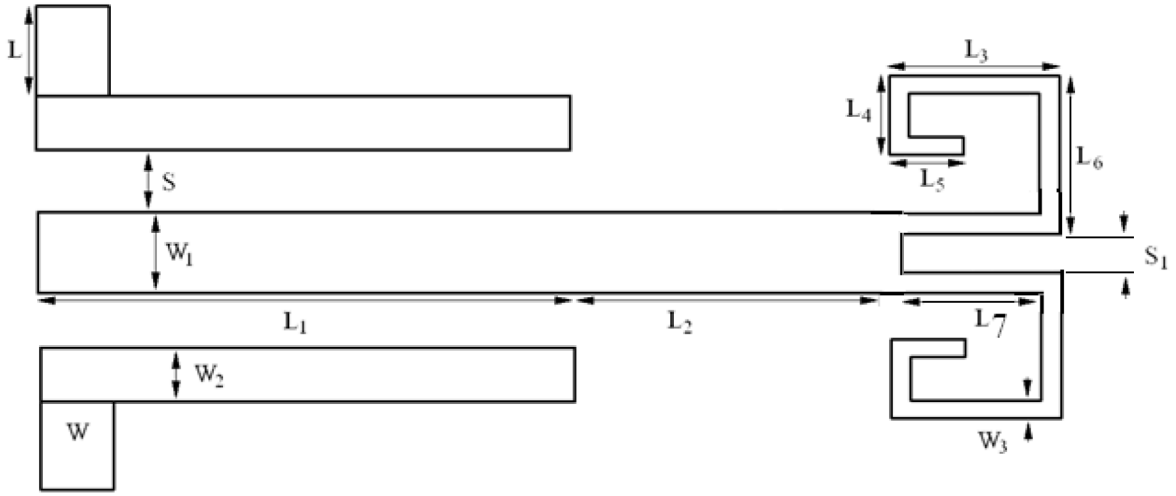

Figure 12. Structure of the broadband band-pass filter with notch. L = 2.2 mm, L_1 = 12 mm, L_2 = 3.4 mm, L_3 = 1.6 mm, L_4 = 0.5 mm, L_5 = 0.4 mm, L_6 = 1.4 mm, L_7 = 1.2 mm, W = 2.2 mm, W_1 = 0.3, W_2 = 0.28 mm, W_3 = 0.2, S = 0.1 mm, S_1 = 0.1 mm.

After selecting the optimized values for the filter parameters, its structure is taken to the program workspace. Figure 13 shows the structure of the designed broadband band-pass filter in the workspace of ADS.

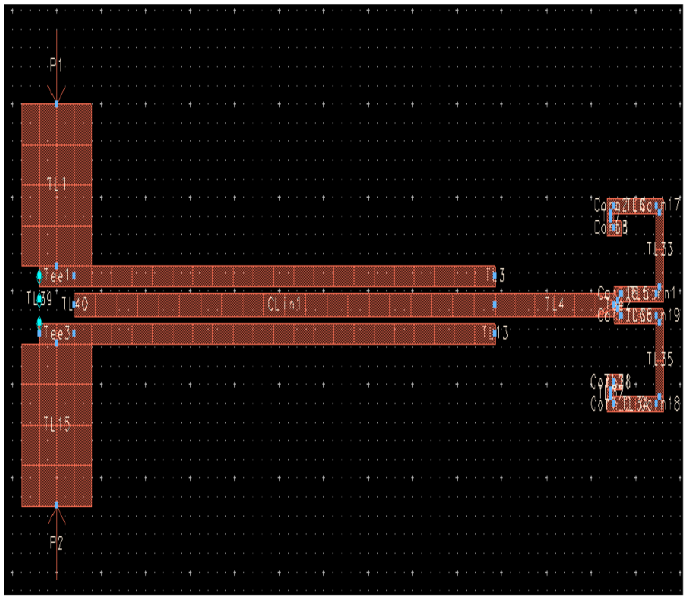

Figure 13. Structure of the broadband band-pass filter.

After implementing the filter in the workspace of ADS, the structure of this filter is implemented on a substrate with a thickness of 0.787 mm and a dielectric constant of 2.2 and the frequency response is simulated in the range of 0–16 GHz.

As observed in Figure 14, this filter gives us a large bandwidth and also the group delay of this band-pass filter is constant in its pass-band.

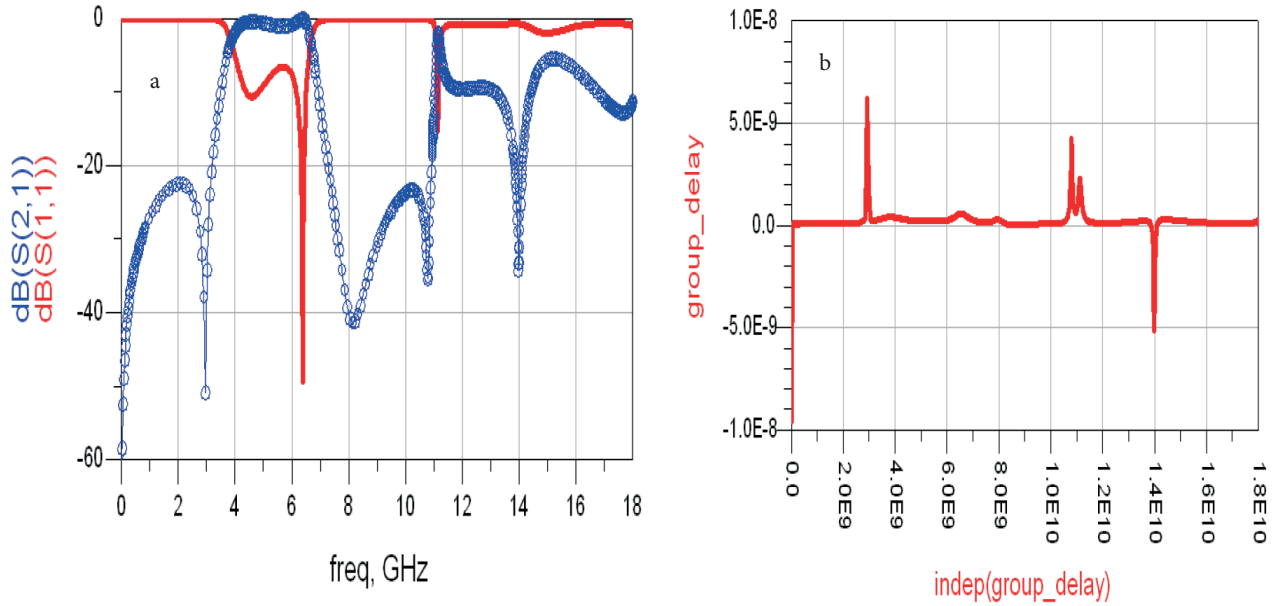

Figure 14. Frequency response of the simulated filter in the ADS program versus a) return losses (S_{11}) and insertion losses (S_{21}) in the range of 0–16 GHz and b) filter phase delay.

4. Ultrawideband band-notched band-pass filter

If the two band-pass filters in the block-diagram of Figure 15 (BPF1 and BPF2) are replaced with the resonators of Figures 11 and 12, then an ultrawideband band-pass filter with a notch-band in its pass-band can be designed.

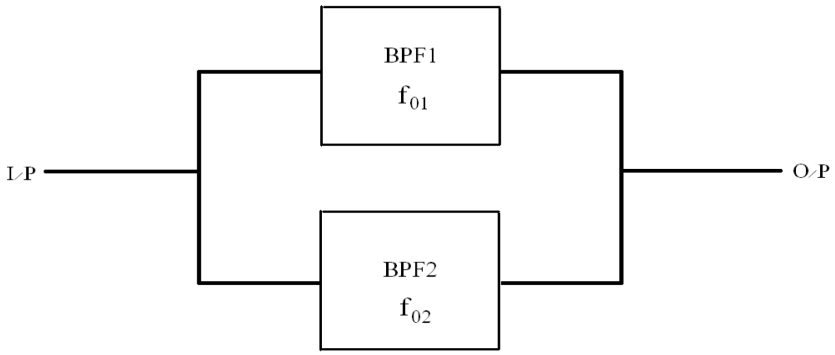

Figure 15. Proposed structure for the design of a band-pass filter with an ultrawide bandwidth.

The structure of the ultrawideband band-pass notch filter given in Figure 16 was transferred to the layout workspace. The the substrate of the filter was specified like the previous filter with a thickness of 0.787 mm and dielectric constant $\varepsilon_r = 2.56$, and finally its frequency response was simulated in terms of transmission and return losses. Their plots are shown in Figure 17.

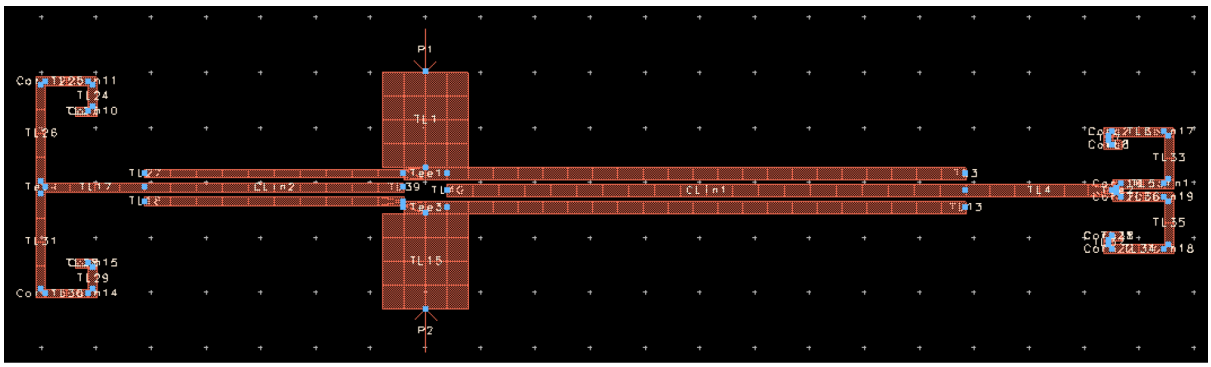

Figure 16. Structure of this ultrawideband band-pass filter in the workspace of ADS.

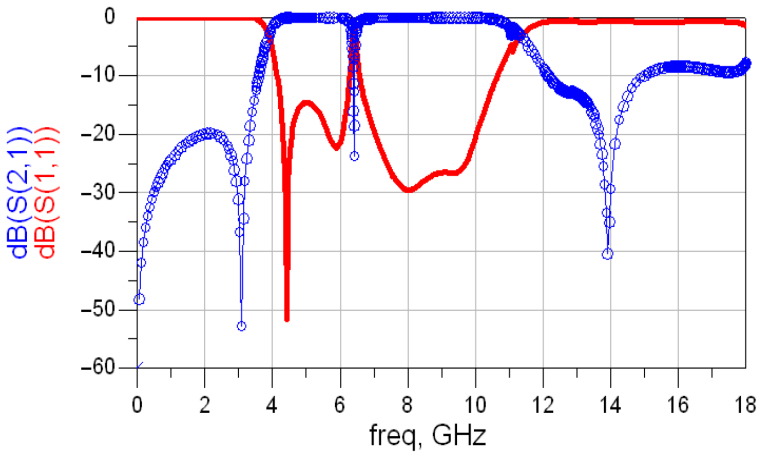

Figure 17. Frequency response of the ultrawideband band-pass filter with notch.

5. Reduced ultrawideband band-pass filter

As indicated in the aforementioned sections, one can design an ultrawideband band-pass filter with notched band using the proposed model. The proposed filter leads to a desirable solution; however, its size is still large. In this part, the size and volume of the band-pass filter is decreased by the use of a resonator, by folding the resonator, and by changing the coupling structure. Figure 18 depicts this ultrawideband band-pass filter with the proposed notch for size purposes in which the coupling structure is varied and the SIR is folded internally in order to reduce the size and volume.

Once this filter's structure is implemented in ADS, similar to the ultrawideband band-pass filter with notch in previous sections, this filter's structure is also optimized based on its parameters. Figure 19 shows the compact ultrawideband filter.

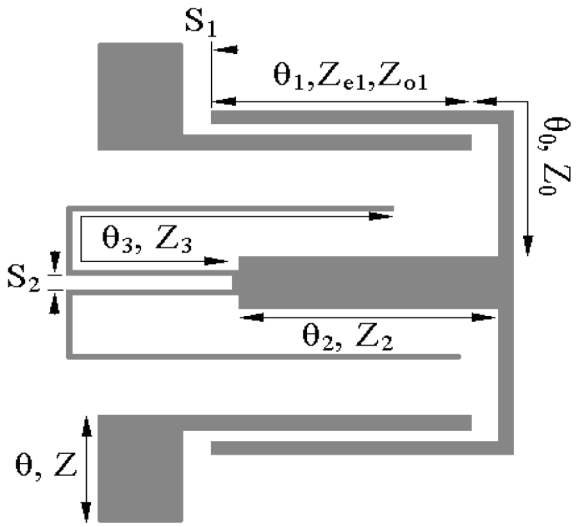

Figure 18. Structure of ultrawideband band-pass filter with notch. $\theta_0 = 18.6$, $\theta = 24.37$, $\theta_1 = 73.4$, $\theta_2 = 51.8$, $\theta_3 = 121.7$, $Z_0 = 60.4\ \Omega$, $Z = 147.5\ \Omega$, $Z_2 = 78.5\ \Omega$, $Z_3 = 170\ \Omega$, $S_1 = 0.3$ mm, $S_2 = 0.2$ mm.

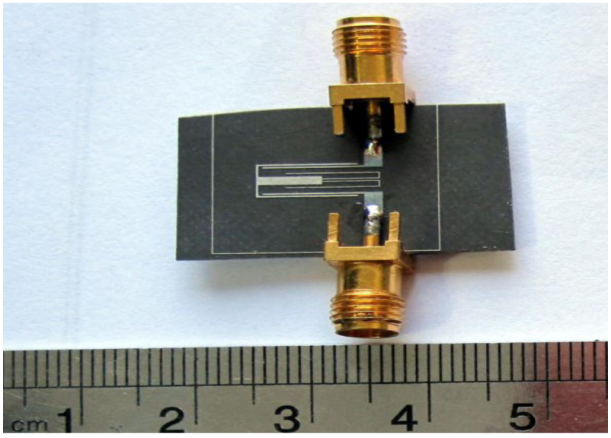

Figure 19. Fabricated picture of the compact ultrawideband filter.

After implementation of the filter, its performance is tested against scattering parameters, transferring loss, and returned loss. Figure 20 illustrates frequency responses related to both simulated and measured reduced ultrawideband band-pass filters with the proposed notch.

As shown from the comparison between simulated and measured frequency responses, these frequency responses correlate with each other very well. Comparison between the frequency responses of this filter and other filters that have been proposed in recent years [10,11] shows its high performance.

6. Conclusion

In this paper, before simulating the filter, its structure was analyzed and the existence and location of transfer zeros were determined and presented. In the new structure it was shown theoretically that, using the transfer zeros, the frequency response of these filters and thus their selectivity can be improved. Moreover, the proposed resonator was improved and another type of this resonator was developed to create a stop-band or notch. According to the structure of these two resonators, a parallel structure was proposed and presented. Finally, using the resonators, a reduced ultrawideband band-notched band-pass filter was designed and proposed. The

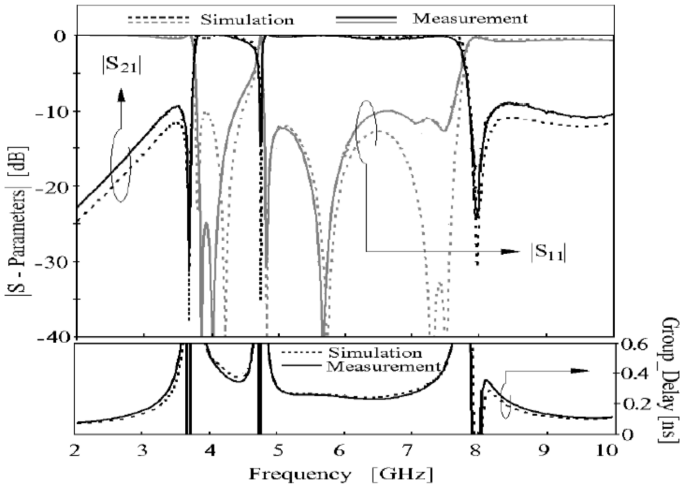

Figure 20. Frequency responses of simulated and measured reduced ultrawideband band-pass filter with notch.

band-notch function was introduced to the filter response by employing a meander embedded open stub on the main resonator and without any increase in the size or price of the filter. The proposed filter is small, has a simple structure, and is easy to be fabricated. The measured results were in good agreement with the simulation predictions and reveal that the proposed filter is a good candidate for ultrawideband applications.

References

[1] Lee CH, Hsu CIG, Chen LY. Notch-bands ultra-wideband bandpass filter design using combined modified quarter-wavelength tri-section stepped-impedance resonators. IET Microw Antennas Propag 2009; 3: 1232-1236.

[2] Huang F. Quasi-dual-mode microstrip spiral filters using first and second harmonic resonances. IEEE T Microw Theory 2006; 54: 742-747.

[3] Lee HM, Tsai CM. Improved coupled-microstrip filter design using effective even-mode and odd-mode characteristic impedances. IEEE T Microw Theory 2005; 53: 2812-2818.

[4] Wang H, Chu QX, Gong Q. A compact wideband microstrip filter using folded multi-mode resonator. IEEE Microw Wirel Co 2009; 19: 287-289.

[5] Li R, Zhu L. Compact UWB bandpass filter using stub-loaded multiple-mode resonator. IEEE Microw Wirel Co 2007; 17: 40-42.

[6] Mao SG, Chueh YZ, Chen CH, Hsieh MC. Compact ultra-wideband conductor-backed coplanar waveguide bandpass filter with a dual band-notched response. IEEE Microw Wirel Co 2009; 19: 149-151.

[7] Yang GM, Jin R, Vittoria C, Harris VG, Sun, NX. Small ultra-wideband (UWB) bandpass filter with notched band. IEEE Microw Wirel Co 2008; 18: 176-178.

[8] Shaman H, Hong, JS. A novel ultra-wideband (UWB) bandpass filter (BPF) with pairs of transmission zeroes. IEEE Microw Wirel Co 2007; 17: 121-123.

[9] Gao J, Zhu L, Menzel W, Bogelsack F. Short-circuited CPW multiple-mode resonator for ultra-wideband (UWB) bandpass filter. IEEE Microw Wirel Co 2006; 16: 104-106.

[10] Valizade A, Rezaei P, Nourinia J, Ghobadi CH, Mohammadi B. An ultra-wideband band-pass filter with band-notch performance based on meander embedded open-circuited stub structure. In: 7th International Symposium on Telecommunications; 2014. pp. 270-273.

[11] Saini Y, Kumar M. Design and analysis of compact UWB bandpass filter with wide passband using defected ground structure. American Journal of Engineering Research 2014; 3: 267-272.